Residue Accessibility, Hydrogen Bonding, and Molecular Recognition: Metal−Chelate Probing of Active Site Histidines in Chymotrypsins[†]

Patrick P. Berna,[‡,§] Nadir T. Mrabet,*[,||] Jozef Van Beeumen,[⊥] Bart Devreese,[⊥] Jerker Porath,[§] and Mookambeswaran A. Vijayalakshmi*[,‡]

Laboratoire d'Interactions Moléculaires et de Technologie de Séparation, Université de Technologie de Compiègne, URA-CNRS 1442, Compiègne, France, ARL Division of Biotechnology and Department of Biochemistry, University of Arizona, Tucson, Arizona 85721, Faculté des Sciences, Université Henri Poincaré−Nancy I, Vandœuvre-lès-Nancy, France, and Department of Biochemistry, Physiology, and Microbiology, State University of Gent, Gent, Belgium

Received July 22, 1996; Revised Manuscript Received November 13, 1996[⊗]

ABSTRACT: Subspecies defining the maturation pathway of bovine chymotrypsinogen to α-chymotrypsin have been separated in a single chromatographic run by affinity to iminodiacetic acid−Cu(II) [IDA−Cu(II)] immobilized onto Novarose. A major highlight of the elution pattern is that, as maturation proceeds, these subspecies exhibit a correlated increase in affinity toward IDA−Cu(II). This behavior is analyzed by a combination of physicochemical and molecular modeling techniques to assess the contribution of the two histidines present in chymotrypsins, at positions 40 and 57 on the protein surface. Catalytic His-57 features adequate surface accessibility to serve as a ligand to IDA−Cu(II), but its participation is clearly ruled out by specific chemical modification. In contrast, His-40, whose side chain is buried in the crystal structures of both zymogen and mature enzyme, surprisingly proves the most plausible candidate as an electron donor to IDA−Cu(II). This apparent conflict between histidine accessibility and their implication in IDA−Cu(II) recognition has been rationalized on the basis of their flexibility and/or hydrogen-bonding status, with the following outcome. First, histidine constitutes a useful reporter group for subtle protein conformational fluctuations. Second, *static* accessibility computation alone provides no unequivocal guideline as to whether a protein residue can serve as a ligand. Third, this study is the first to document the occurrence of a screening effect due to hydrogen bonding of an otherwise "accessible" histidine. A significant corollary to this finding would be that the catalytic histidine is rigidly entrapped in a remarkably strong hydrogen-bonding network, a situation that may pertain to mechanistic aspects of catalysis.

Probing protein surface topography traditionally relies on molecular modeling of *static, heavy atom* protein models obtained by X-ray crystallography. Dynamic aspects of conformation in solution are hence not readily acknowledged. Similarly, X-ray models contain no factual information about the strength of hydrogen-bonding interactions. We here illustrate the occurrence of both situations and demonstrate the utility of the concurrent analysis of the protein in solution by means of a small affinity probe, the metal−chelate complex, iminodiacetic acid−Cu(II) [IDA−Cu(II)], which exhibits a unique specificity to protein surface-accessible histidines near neutral pH (Sulkowski 1985, 1987, 1989; Mrabet, 1992).

Two decades ago, Porath first introduced immobilized metal affinity chromatography (IMAC;[1] Porath et al., 1975), a technique that takes advantage of the property of a few amino acids to bind chelated transition metal ions, as a purification method for biological molecules. In IMAC, metal ions are immobilized by complex formation with a metal-chelating agent which is, itself, covalently attached to a hydrophilic support. When a protein mixture is percolated through an IMAC column, some proteins, which carry on their external surface amino acid residues with electron donor character, can bind to the chelated metal through the available coordination sites, and are hence adsorbed, while others elute from the column unretarded. On the basis of this principle, applications of IMAC range from the separation of small molecules such as amino acids (Fazakerley & Best, 1965), nucleotides (Hubert & Porath, 1981), or aromatic amines (Liu & Yu, 1990) to the purification of a variety of proteins (Sulkowski, 1985), including membrane glycoproteins (Corradini et al., 1988) and engineered proteins bearing synthetic metal affinity sites on their surface [for a review, see Arnold (1991)], and even further extend to the separation of intact cells (Botros & Vijayalaksmi, 1989). Moreover, the potential

[†] This research was supported in part by grants from the Flemish government for the Concerted Research Action Program (J.V.B.) and the Carl Trygger Foundation (J.P.) and by financial support provided by Prof. J. Law, Biotechnology Department, University of Arizona, Tucson, to P.B.

* Corresponding authors. M.A.V.: phone, (33) 344 23 44 04; Fax, (33) 344 20 39 10; E-mail, viji@utc.fr. N.T.M.: phone, (33) 383 91 24 98; Fax, (33) 383 91 20 93; E-mail, n.mrabet@gauguin.legg.u-nancy.fr.

[‡] Université de Technologie de Compiègne.

[§] University of Arizona.

[||] Université Henri Poincaré−Nancy I.

[⊥] University of Gent.

[⊗] Abstract published in *Advance ACS Abstracts,* May 1, 1997.

[1] Abbreviations: ASA, accessible surface area; BAEE, N^{α}-benzoyl-L-arginine ethyl ester; BTEE, *N*-benzoyl-L-tyrosine ethyl ester; CGA, bovine chymotrypsinogen; CHA, bovine α-chymotrypsin; DFP, diisopropyl fluorophosphate; ES-MS, electrospray ionization mass spectrometry; H-bond, hydrogen bond; IDA, iminodiacetic acid; IMA, immobilized metal affinity; IMAC, immobilized metal affinity chromatography; MES, 2-(*N*-morpholino]ethanesulfonic acid; MNBS, methyl-4-nitrobenzene sulfonate; MOPS, 3-(*N*-morpholino)propanesulfonic acid; Novarose, Novarose Act^{High}-100/40; PDB, Protein Data Bank; PMSF, phenylmethanesulfonyl fluoride; RMS, root mean square; SD, standard deviation; TPCK, *N*-tosyl-L-phenylalanine chloromethyl ketone.

S0006-2960(96)01807-7 CCC: $14.00

for high resolution of metal-based affinity purification has been previously demonstrated by the separation in a single chromatographic run of recombinant D-xylose isomerase from a crude cell lysate (Mrabet, 1992) or of 19 peptide hormones, some of which differ in their primary sequence only by the configuration (L or D) of a single amino acid (Nakagawa et al., 1988). The name "Porath's triad" was coined by Sulkowski in recognition of the pioneering work of Porath (Porath et al., 1975) to designate the amino acids most likely involved in IMAC, histidine, tryptophan, and cysteine (Sulkowski, 1985, 1989). Furthermore, Sulkowski was able to document a mechanistic link between histidine topography and protein binding selectivity in IMAC (Sulkowski, 1987, 1989; Hemdan et al., 1989; Zhao et al., 1991). Using a multidisciplinary protein engineering approach, Mrabet was recently able to provide a direct demonstration of histidine implication in IMAC near neutral pH and to address the prominent issue of residue accessibility in metal−chelate recognition (Mrabet, 1992).

Bovine chymotrypsin (E.C. 3.4.21.1) is a member of the serine protease family which contains only two histidines at positions 40 and 57, both located on the protein surface. His-57 belongs to the catalytic triad, while His-40 is located near the edge of the active site. Chymotrypsinogen, the nonactive precursor and storage form of the enzyme, is activated by tryptic cleavage of the bond between Arg-15 and Ile-16 (Dreyer & Neurath, 1955) to produce π-chymotrypsin; subsequent autocatalytic hydrolysis of three other peptide bonds gives rise to the δ, κ, and α or γ forms of the enzyme (Rovery et al., 1955). Sulkowski has previously shown that chymotrypsinogen and α-chymotrypsin behaved differently on Chelating Sepharose−IDA−Cu(II) (Sulkowski, 1987). At pH 7, the zymogen did not bind to the metal−chelate complex, whereas α-chymotrypsin was retained and could subsequently be eluted by lowering the pH to 6. Moreover, chemical modification of active site Ser-195 with diisopropyl fluorophosphate (DFP) in α-chymotrypsin produced a stronger interaction to IDA−Cu(II). To explain this behavior, Sulkowski suggested the occurrence of a major alteration in the microenvironment of nearby His-57, the presumed protein ligand, with induced changes in the accessibility and/or pK_a of this residue (Sulkowski, 1987).

In the present study, alteration of the microenvironment of histidine residues during the process of maturation from chymotrypsinogen to δ-, κ-, and α- or γ-chymotrypsin is indeed shown to promote changes in protein affinity to immobilized IDA−Cu(II). These findings are analyzed by a combination of biochemical techniques and molecular modeling of the high-resolution crystal structures of the proteins to reveal that surface histidine can serve as an exquisite reporter group for subtle conformational changes which are not readily foreseeable by examination of X-ray crystallographic protein models and to further provide evidence for the occurrence of remarkably strong hydrogen bonds at the protein surface and for their implication as a determinant to metal−chelate recognition.

EXPERIMENTAL PROCEDURES

Materials

Bovine chymotrypsinogen C4879 (lot 39F8095), δ-chymotrypsin C9381 (lot 68F8075), γ-chymotrypsin C4754 (lot 30H8065), α-chymotrypsin C4129 (Lots 61H7175, 100H8275, and 71H7071), DFP-treated α-chymotrypsin C1012 (lot 54F8145), bovine serum albumin (fraction V), copper sulfate·5H_2O, diisopropyl fluorophosphate (DFP), phenylmethanesulfonyl fluoride (PMSF), ethylenediaminetetraacetate disodium salt (EDTA), *N*-benzoyl-L-tyrosine ethyl ester (BTEE), N^{α}-benzoyl-L-arginine ethyl ester (BAEE), imidazole, *N*-tosyl-L-phenylalanine chloromethyl ketone (TPCK), methyl 4-nitrobenzene sulfonate (MNBS), iminodiacetic acid (IDA), 2-(*N*-morpholino)ethanesulfonic acid (MES), and 3-(*N*-morpholino)propanesulfonic acid (MOPS) were obtained from Sigma Chemical Co. (St. Louis, MO). All chemicals used were of reagent grade. Desalting PD 10 columns were from Pharmacia (Uppsala, Sweden). The chromatographic matrix Novarose Act^{High}-100/40 was a gift from Inovata AB (Bromma, Sweden). Ultrapure water obtained with the MilliRO−MilliQ+ system (Millipore) was used throughout.

Methods

Matrix Derivatization. Iminodiacetic acid (IDA) was directly coupled to the activated, new agarose-based media, Novarose Act^{High}-100/40 (henceforth designated Novarose), as follows. One hundred grams of Novarose were washed, suction drained, and then mixed with 100 mL of 1 M Na_2CO_3 containing 1 M IDA at pH 12. The suspension was mechanically shaken for 24 h at room temperature, and the coupling reaction was stopped by washing the gel with distilled water until a neutral pH was reached. Eventual residual activated groups in the resin were hydrolyzed by heating the gel at 80 °C for 30 min. For Cu(II) capacity measurement, the column was first loaded with 50 mM $CuSO_4$ in 50 mM sodium acetate, pH 4.5, and then washed with 100 mM imidazole, pH 7; bound Cu(II) was finally eluted with 50 mM EDTA, and its concentration in the eluate was determined by atomic absorption spectrometry. This yields a capacity value of 120 μmol of Cu(II)/mL of gel bed, which is in the expected range for Novarose (technical note, Inovata).

General Chromatographic Procedures. All chromatographic procedures were carried out at room temperature with a low-pressure liquid chromatography system (EconoSystem, Bio-Rad, Richmond, VA). A 1 × 4 cm column was used at a linear flow rate of 15.3 cm/h, and protein elution was followed by monitoring the absorbance at 280 nm. The Novarose-IDA column was saturated with 50 mM $CuSO_4$ in water, subsequently washed with water, and finally equilibrated with the adsorption buffer (30 mM Tris-HCl, pH 7.5, 1 M NaCl; buffer A). This buffer was used to dissolve the commercial lyophilized protein to a concentration of 10 mg of protein in 0.5 mL, and this sample was applied onto the column. Fractions of 1.4 mL were collected and analyzed for chymotryptic activity using *N*-benzoyl-L-tyrosine ethyl ester (BTEE) (Hummel, 1959), for tryptic activity using N^{α}-benzoyl-L-arginine ethyl ester (BAEE) (Schwert & Takenaka, 1955), and for protein content using the Bradford assay (Bradford, 1976). After each run, the gel was regenerated by flushing with 5 column volumes of 50 mM EDTA and thoroughly washed with water before a new metal load was applied.

Chromatographic Separation of Bovine Chymotrypsin Subspecies. Prior to chromatography, the Novarose−IDA−Cu(II) was thoroughly equilibrated with buffer A. The commercial bovine α-chymotrypsin sample (Sigma C4129, lot 61H7175, 100H8275, or 71H7071) was applied, and the

gel washed with 4 bed volumes of buffer A. A discontinuous, increasing concave gradient was applied by mixing buffer A and buffer B (100 mM Tris-HCl buffer, pH 7.5, 1 M NaCl) as follows: 0 min, 100% A, 0% B; 100 min, 93% A, 7% B; 200 min, 78% A, 22% B; 300 min, 50% A, 50% B; 400 min, 0% A, 100% B; 500 min, 0% A, 100% B. The gel was finally washed with the adsorption buffer containing 100 mM imidazole. The eluted fractions were immediately analyzed for activity and protein content and finally supplemented with phenylmethanesulfonyl fluoride (PMSF) (Farhney & Gold, 1963) to a final concentration of 1 mM.

Characterization of Chymotrypsin Subspecies by Electrospray Mass Spectrometry. The PMSF-inhibited fraction corresponding to the center of each peak was desalted and mixed with 50% acetonitrile and 1% formic acid in water prior to positive ion electrospray mass spectrometry analysis on a Bio-Q triple quadrupole analyzer (Fisons).

Affinity Labeling of Active Site Residues. Affinity labeling of His-57 with *N*-tosyl-L-phenylalanine chloromethyl ketone (TPCK) or methyl 4-nitrobenzenesulfonate (MNBS) was carried out according to Schoellmann and Shaw (1963) and Nakagawa and Bender (1970), respectively. Ser-195 was affinity labeled with PMSF as described by Farhney and Gold (1963). In each case, inhibition reached at least 95% completion. Excess reagent was removed by desalting prior to chromatography. Inhibition was found to remain unchanged even after a chromatographic run. DFP-treated α-chymotrypsin (C1012, lot 54F8145) was purchased directly from Sigma Chemical Co. (St. Louis, MO).

Nonchromatographic Equilibrium Binding Analysis. Nonchromatographic equilibrium binding analysis was done in a similar way to that described by Hutchens (1990). The experiment was carried out at room temperature (20−22 °C). Novarose−IDA−Cu(II) was equilibrated with buffer A and then allowed to settle in a 10-mL graduated cylinder to a constant bed volume. The gel was then homogeneously suspended after addition of an equal volume of buffer A, and 200-μL aliquots of the suspension (equivalent to 100 μL of settled gel) were added to a series of Eppendorf tubes, in triplicate, containing 100 μL of α-chymotrypsin at varying concentrations in buffer A. Lot 71H7071 used in this experiment represents more than 85% α- or γ-chymotrypsin as analyzed by chromatography on Novarose−IDA−Cu(II). After a 30 min incubation with intermittent shaking, the tubes were centrifuged and a 100 μL aliquot of the supernatant was withdrawn from each tube to determine the unbound protein concentration, [P]. The ligand-bound protein concentration, [PL], was determined from the difference between the initial protein concentration, [P_0], and unbound protein concentration, [P]. The data, [PL], were plotted as a function of [P] according to the Langmuir adsorption isotherm, while the data, [PL]/[P], were plotted as a function of [PL] according to Scatchard (1949). Curve fitting and parameter determination were done with the SigmaPlot software from Jandel Scientific.

pH Titration. pH titration was performed as described previously by Sulkowski (1987). A three-component mixture containing equimolar amounts (20 mM each) of MOPS (pK_a 7.15 at 25 °C), MES (pK_a 6.09 at 25 °C), and acetic acid (pK_a 4.76 at 25 °C) was used as the chromatography buffer with pH adjusted to the desired value with 10 N NaOH [all pK_a values are from Perrin and Dempsey (1987)]. The protein sample of chymotrypsin was chromatographed isocratically at various pH values as indicated in Figure 2A. The sample lot used was Sigma 100H8275 which consisted of ∼45% α- or γ-chymotrypsin as analyzed by chromatography on Novarose−IDA−Cu(II).

Molecular Modeling. Accessible surface area (ASA; Å^2) computation was done starting with heavy atom protein crystal models corresponding to Brookhaven Protein Data Bank (PDB; Bernstein et al., 1977) entries 2CGA (crystal resolution = 1.8 Å; residual *R*-factor = 0.173) for bovine pancreatic chymotrypsinogen (Wang et al., 1985) and 5CHA (crystal resolution = 1.67 Å; residual *R*-factor = 0.179) for bovine α-chymotrypsin (Blevins & Tulinsky, 1985), according to the following procedure. Hydrogen atoms were constructed on the heavy atom structures and their positions modeled as described further below. Each protein structure was subsequently energy minimized, so as to regularize bond distances and angles and to relieve close contacts, using 500 steps of steepest descent minimization (Levitt & Lifson, 1969), with all the atoms of the system, including aliphatic and polar hydrogens, being considered explicitly. Forces and interaction energies between all atoms were calculated using the CHARMm potentials (Brooks et al., 1983) implemented in the BRUGEL molecular modeling package (Delhaise et al., 1984; UsrConsult, Louvain-la-Neuve, Belgium) on a INDIGO^2 Extreme Silicon Graphics station. The resulting structures present root mean square (RMS) deviations averaged over all protein heavy atoms that are very small, with values of 0.226 Å for PDB entry 2CGA and 0.289 Å for PDB entry 5CHA, indicative of overall energetically adequate atom positioning in the original X-ray structures. ASA computation was subsequently done on each minimized structure, after removal of all hydrogen atoms, that is while considering only the heavy atoms. For this purpose, the protein atom radii used are of the united type and correspond to those of Brooks et al. (1983). ASA values to the 1.93-Å radius probe sphere, mimicking IDA−Cu(II) (Mrabet, 1992), were calculated with the analytical procedure SurVol (Alard, 1991; Alard & Wodak, 1991) implemented in BRUGEL.

Hydrogen bonding was computed in all hydrogen atom molecules starting with Brookhaven PDB entries 2CGA and 5CHA, as follows. After energy minimization as described above, all hydrogen atoms were "eliminated", keeping only the structures' heavy atoms. New hydrogen atoms were then constructed and their positions optimized using the steepest descent minimization algorithm (Levitt & Lifson, 1969) implemented in BRUGEL, while applying full constraint on the protein heavy atoms. Hydrogen bonds were modeled as previously described (Wodak et al., 1995).

RESULTS AND DISCUSSION

Distinct Chromatographic Behavior of Chymotrypsin Subspecies on IDA−Cu(II). IDA−Cu(II) immobilized metal affinity chromatography of commercial samples of α-chymotrypsin is found to reproducibly result in an elution pattern containing five peaks (Figure 1A). The flowthrough, unbound protein peak is designated peak I. Elution with a Tris-HCl gradient from 30 to 100 mM generates three separate peaks, numbered II−IV. The final washoff step with 100 mM imidazole finally elutes a fifth minor protein peak (peak V). Peaks II−IV all display chymotryptic activity, whereas peaks I and V do not. No tryptic activity could be detected in any of the peaks. To characterize the different chymotrypsin subspecies and test whether some of the peaks could represent aged products, they were further

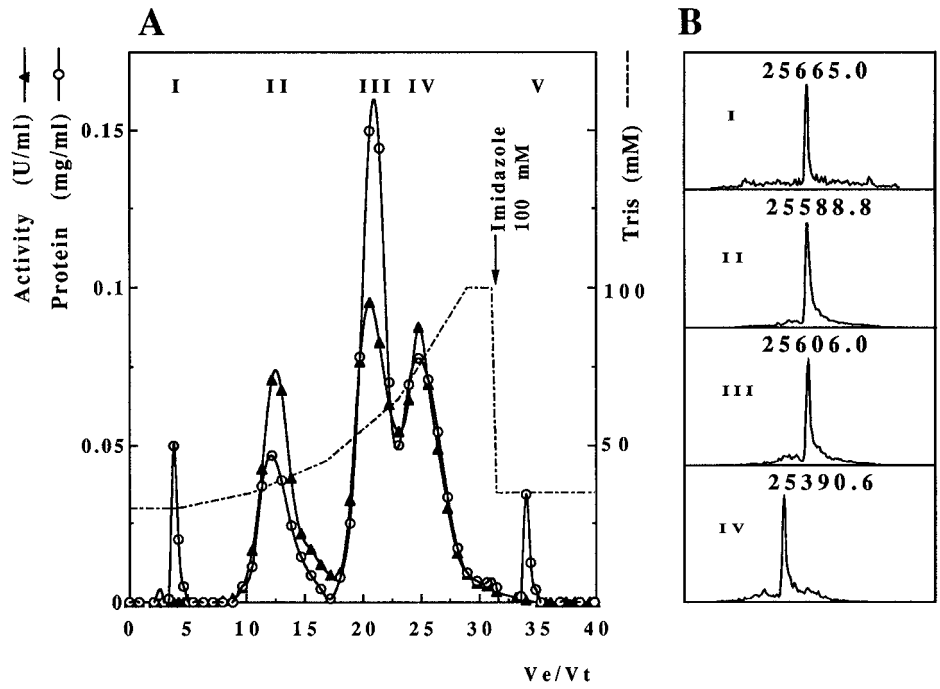

FIGURE 1: Chromatographic separation of bovine chymotrypsin subspecies on Novarose−IDA−Cu(II) and characterization by electrospray mass spectrometry. (A) Chromatographic profile of a commercial sample of bovine α-chymotrypsin on Novarose−IDA−Cu(II). Protein peak I elutes in the flowthrough. A Tris gradient allows separation of three protein peaks numbered II−IV. A washoff step of 100 mM imidazole is finally used to elute a fifth minor protein peak (peak V). Peaks II−IV all display chymotryptic activity, whereas peaks I and V do not. No tryptic activity can be detected in any of the peaks. (B) Analysis by electrospray mass spectrometry of the chromatographic fractions following inactivation with PMSF. The positive ion electrospray mass spectra indicate that the components in peaks I−IV are homogeneous and have discrete molecular weights. The mass value for peak I (25665.0 Da) corresponds to the theoretical molecular mass of chymotrypsinogen (25656.1 Da), the mass of the second peak (25588.8 Da) to the theoretical mass of PMSF−δ-chymotrypsin (25586.1 Da), the mass of peak III (25606.0 Da) to the theoretical mass of PMSF−κ-chymotrypsin (25605.1 Da), and the mass of the fourth peak (25390.6 Da) to the theoretical masses of PMSF−α- or PMSF−γ-chymotrypsin (25389.9). Peak V contains degradation products and inactive chymotrypsin subspecies that most likely correspond to denatured or degraded enzymes. The ion electrospray spectrum of the commercial sample reveals the presence of the four chymotrypsin subspecies (data not shown).

analyzed by positive electrospray ionization mass spectrometry (ES-MS). For this purpose, the peak fractions were first treated with PMSF to eliminate eventual proteolytic autodegradation. The ES-MS analysis indicates that the components in peaks I−IV are homogeneous and have discrete molecular weights. The mass value for peak I (25665.0 Da) corresponds to the theoretical molecular mass of bovine chymotrypsinogen (25656.1 Da), the mass of the second peak (25588.8 Da) to the theoretical mass of PMSF−δ-chymotrypsin (25586.1 Da), that of peak III (25606.0 Da) to the theoretical mass of PMSF−κ-chymotrypsin (25605.1 Da), and finally, the mass of the fourth peak (25390.6 Da) to the theoretical masses of PMSF−α- or PMSF−γ-chymotrypsin (25389.9 Da) (Figure 1B). The nature of peak IV could not be specified any further as ES-MS cannot distinguish between α- and γ-chymotrypsins which have identical molecular masses.[2] Peak V, which represents less than 3% of the total protein sample and exhibits the highest affinity to IDA−Cu(II), is heterogeneous as it contains a mixture of molecules with molecular masses ranging from 1500 to 25673 Da. Since peak V is totally devoid of any chymotryptic activity or PMSF reactivity, it hence most likely consists of a mixture of degraded and unfolded chymotrypsins.

To our knowledge, this is the first report of a successful separation of all four chymotrypsin subspecies in a single chromatographic run. We propose that this result is the consequence of enhanced selectivity engineering in IMAC, which itself is the consequence of the combined use of a high copper density matrix (see below) and of Tris-HCl as a mild competitor. Indeed, the weaker competitive effect of the Tris-HCl molecule toward the chelated metal ion, as compared to the usual imidazole competitor, is expected to provide for the generation of an effectively "shallow" gradient and hence for a fine-tuned elution, therefore further increasing the resolution power of IMAC. Moreover, the new chelating agarose gel used in this study, Novarose−IDA, has a ligand density that is four times higher than previous commercial IDA chelating gels, and this parameter is likely to also contribute, on a gel-bed length basis, to an improved resolution of the closely related chymotrypsin subspecies. Furthermore, we also suggest that the high ligand density is responsible for the 7-fold increase in α- or γ-chymotrypsin maximal protein capacity observed for Novarose−IDA−Cu(II) (2.27 μmol or 57 mg of α- or γ-chymotrypsin/mL of wet gel) when compared to Chelating Sepharose Fast Flow−IDA−Cu(II) (7.5 mg of α- or γ-chymotrypsin/mL of wet gel; Hutchens & Yip, 1990).

An attempt to separate an "artificial" mixture of commercial bovine α- (Sigma C4129, lot 61H7175) and γ-chymotrypsin (Sigma C4754, lot 30H8065) subspecies on Novarose-IDA-Cu(II) was unsuccessful. Therefore, their

[2] Recent crystallographic studies have shown that α-chymotrypsin and γ-chymotrypsin are in fact the same subspecies, except that γ-chymotrypsin can occur as a complex, either as a noncovalent or as a covalent tetrahedral adduct to active site Ser-195, of α-chymotrypsin with its own autolysis product, an oligopeptide that can vary in length from three to five residues (Dixon & Matthews, 1989; Harel et al., 1991). This complex formation appears to arise from the lengthy crystallization conditions (Harel et al., 1991) and should hence not be observed under our experimental conditions.

Table 1: Accessible Surface Areas of His-40 and His-57 in Bovine Chymotrypsinogen and α-Chymotrypsin[a]

protein	chymotrypsinogen	α-chymotrypsin	ASA change (%)
His-40 (all atoms)	11.95 ± 1.63	19.55 ± 0.78	63.6
His-40.ND1	0	0	0
His-40.CD2	2.00 ± 1.03	0.98 ± 0.31	−51.0
His-40.CE1	0	0	0
His-40.NE2	0	0	0
His-57 (all atoms)	62.60 ± 0.28	63.30 ± 2.26	1.1
His-57.ND1	0	0	0
His-57.CD2	22.25 ± 2.33	26.75 ± 2.62	20.2
His-57.CE1	0	0	0
His-57.NE2	1.10 ± 1.34	1.26 ± 0.67	14.5

[a] Computation of accessible surface areas (ASA; Å^2; mean per monomer in the "two-monomer-per-unit-cell" crystal structures ± 1 SD) was done using SurVol (Alard, 1991; Alard & Wodak, 1991) on heavy atom protein models using a spherical probe radius of 1.93 Å, which mimics IDA−Cu(II) (Mrabet, 1992). These protein models were derived by geometrical optimization of the Brookhaven PDB (Bernstein et al., 1977) entries 2CGA for bovine pancreatic chymotrypsinogen (Wang et al., 1985) and 5CHA for bovine α-chymotrypsin (Blevins & Tulinsky, 1985) using the steepest descent energy minimization protocol (Levitt & Lifson, 1969). Other details are provided in Experimental Procedures.

coelution as a single protein peak can reasonably be interpreted as the occurrence of identical interacting sites for IDA−Cu(II).[2]

Our results further indicate that the commercial enzyme consists of a mixture of all subspecies that define the maturation pathway of chymotrypsinogen, except π-chymotrypsin which could not be identified. Note that we also confirm the previous observation that active α-chymotrypsin (CHA) but not the zymogen (CGA) is retained on IDA−Cu(II) (Sulkowski, 1987). Furthermore, we observe an intriguing correlation that certainly deserves consideration: the IMAC elution profile shown in Figure 1 indicates that the enzyme affinity for IDA−Cu(II) increases as maturation proceeds. Such a chromatographic behavior is classically interpreted to signify a parallel increase in histidine exposure on the protein surface and would therefore suggest that the accessibility of His-40 and/or His-57 augments during the course of chymotrypsin activation.

Accessibility of Histidine Residues. Computation of histidine accessibility to IDA−Cu(II) in CGA and CHA was performed using the rolling sphere approach (Lee & Richards, 1971) by means of the analytical procedure SurVol (Alard, 1991; Alard & Wodak, 1991) with a probe radius of 1.93 Å which mimics the IDA−Cu(II) ligand, as described previously (Mrabet, 1992). This analysis indicates that the most exposed histidine is clearly His-57, whose ASA remains unchanged at a value of ∼63 Å^2 in both chymotrypsinogen and chymotrypsin (Table 1 and Figure 3). In contrast, His-40 is less exposed with an ASA of ∼12 Å^2 in CGA and ∼20 Å^2 in CHA. The "all-atoms" accessibility data in Table 1 therefore brings no clue to the differential affinity mechanism displayed by chymotrypsin subspecies in IMAC. Moreover, the availability of an accessible His-57 in chymotrypsinogen appears to contradict its observed lack of binding to IDA−Cu(II). We, therefore, attempted to clarify this issue by further determining the accessibility of each atom in histidine imidazole rings. Potential candidates as electron donor atoms are both nitrogens ND1 and NE2, but because carbon and nitrogen atoms cannot be unequivocally distinguished in a protein crystal structure unless the atomic

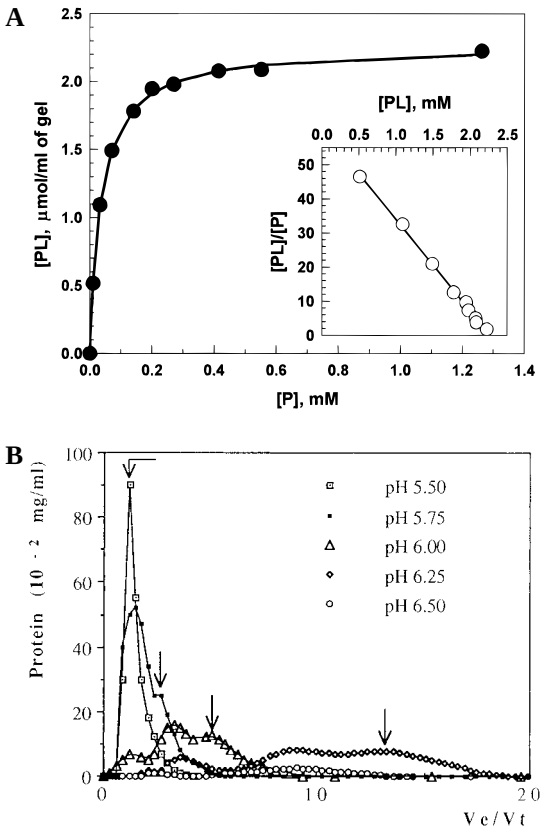

FIGURE 2: Nonchromatographic equilibrium binding analysis and pH titration of α-chymotrypsin on Novarose−IDA−Cu(II). (a) Equilibrium binding analysis was done at room temperature. Incubation of Novarose-IDA-Cu(II) with increasing concentrations of α-chymotrypsin in 30 mM Tris-HCl, pH 7.5, and 1 M NaCl, was carried out in Eppendorf tubes for 30 min with intermittent shaking. After centrifugation to settle the gel, aliquots were withdrawn from the supernatants and used to determine the unbound protein concentration [P]. The ligand-bound protein concentration, [PL], was determined from the difference between the initial protein concentration, [P_0], and the unbound protein concentration, [P]. The data, [PL], is plotted as a function of [P] according to the Langmuir binding isotherm and fitted to the equation $[PL] = B_{max}[P]/(K_d + [P])$ using SigmaPlot; the standard error is 0.0215 μmol/mL and the correlation coefficient is equal to 0.9996; $B_{max} = 2.262$ μmol/mL and $K_d = 37$ μM. The inset shows the data representation according to Scatchard (1949) which yields a straight line (standard error = 0.7971; correlation coefficient = 0.9988) consistent with the occurrence of a single type of binding site under the conditions used. The apparent K_d value is 37 μM while the maximum protein binding capacity is 2.268 μmol/mL of gel (∼57 mg of α- or γ-chymotrypsin/mL of wet gel). (B) The determination of the pK_a range of the interacting site in α/γ-chymotrypsin is based on isocratic chromatography at various pH values from 4.0 to 6.5 using a three-component buffer mixture of equimolar (20 mM each) MOPS, MES, and acetic acid. The elution volume, V_e, of the last peak, which corresponds to α/γ-chymotrypsin (∼45% of total), was measured and is indicated by an arrow in the figure. It is seen that above pH 6.25 protein retention becomes extensive, hence preventing the measurement of V_e. Using the SigmaPlot software, we could, nevertheless, satisfactorily fit the data V_e/V_t vs pH to the pH titration equation $V_e/V_t = a/(1 + 10^{b(pK_a - x)}) + c$ (V_t is the total bed volume) and deduce the following parameters: $a = 46.330$; $b = 2.296$; pK_a = 6.456; $c = 1.604$; standard error = 0.071; correlation coefficient = 0.99995.

resolution is near 1 Å [see McDonald and Thornton (1994)], atom positions CD1 and CE2 were also considered. Table 1 shows that while the total accessibility of His-40 increases (∼64%) with zymogen maturation, that of its imidazole ring instead decreases such that no atom can be available to interact with IDA−Cu(II). Concerning His-57, while the total ASA remains unchanged, we observe a near 15%

Table 2: Hydrogen-Bonding Interactions Made by His-40 and His-57 in Bovine Chymotrypsinogen and α-Chymotrypsin[a]

histidine nitrogen atom protonated	H-bonding partners		chymotrypsinogen			α-chymotrypsin A		
	atom 1	atom 2	dist	θ_1	θ_2	dist	θ_1	θ_2
His-40.ND1	A40.HIS.HD1	A32.SER.OG	1.93	146.3	111.5	1.95	168.5	111.8
	A40.HIS.NE2	*608.HOH.H1*	2.62	139.3	139.4		absent	
	608.HOH.H2	A194.ASP.OD1	2.46	103.6	125.0		absent	
	B40.HIS.HD1	B32.SER.OG	2.04	153.0	122.5		absent	
	B40.HIS.NE2	*718.HOH.H1*	2.12	124.3	150.3		absent	
	718.HOH.H1	B194.ASP.OD1	2.18	117.0	117.8		absent	
	B40.HIS.HD1	B33.LEU.O		absent		2.20	155.1	119.5
His-40.NE2	A40.HIS.HE2	A194.ASP.OD1	1.76	150.6	130.9		absent	
	A40.HIS.HE2	A193.GLY.O		absent		1.72	150.5	133.6
	B40.HIS.HE2	B194.ASP.OD1	1.85	155.2	109.8		absent	
His-57.ND1	A57.HIS.H	A102.ASP.OD1	1.80	152.7	142.9	1.86	164.9	150.3
	A57.HIS.HD1	A102.ASP.OD2	2.05	141.5	101.4	1.96	140.3	104.3
	A57.HIS.NE2	A195.SER.HG	2.56	120.1	92.5	2.54	109.8	111.7
	B57.HIS.H	B102.ASP.OD1	1.89	164.7	141.3	1.88	155.8	147.8
	B57.HIS.HD1	B94.TYR.OH	1.86	130.8	146.0		absent	
	B57.HIS.HD1	B102.ASP.OD2		absent		2.09	116.5	104.2
	B57.HIS.NE2	B195.SER.HG		absent		2.60	120.1	90.5
His-57.NE2	A57.HIS.H	A102.ASP.OD1	1.78	152.0	143.4	1.86	164.9	150.3
	A57.HIS.HE2	A195.SER.OG	1.80	151.0	109.7	2.24	132.8	91.2
	B57.HIS.H	B102.ASP.OD1	1.89	164.7	139.8	1.88	155.9	147.6
	B57.HIS.HE2	B195.SER.OG		absent		1.88	142.8	102.9

[a]Hydrogen bonds are indicated for both bovine chymotrypsinogen and bovine α-chymotrypsin with His-40 and His-57 in either the ND1-protonated form or the NE2-protonated form. In both bovine chymotrypsinogen and bovine α-chymotrypsin, the crystal unit consists of two enzyme molecules, each chain being identified with the prefix A or B. For the sake of simplicity, only H-bonds involving histidine imidazole atoms are indicated; where present, intervening water molecules are indicated in italics and their other hydrogen-bonded protein partner(s) is (are) also specified. Dist is the distance in angstroms between the centers of the hydrogen atom and of the H-bond acceptor atom, while θ_1 and θ_2 designate the bond angles made by donor and acceptor atoms along the H-bond, respectively (linear hydrogen bond has $\theta_1 = 180°$ in this convention; angle and distance cutoffs are 90° and 2.7 Å, respectively). The methodology utilized for hydrogen atom construction and optimization and for hydrogen bond modeling is described in Experimental Procedures. Note that, by considering only the heavy atoms of the protein residues and of the water molecules that intervene in the hydrogen-bonding interactions described here, the RMS deviations between the original PDB entries and the energy-refined structures are very small, with values equal to 0.237 ± 0.018 Å for 2CGA and 0.282 ± 0.007 Å for 5CHA (mean ± 1 SD, taking into account the two protein molecules present in the asymmetric unit of the crystal structures).

increase in the ASA of His-57.NE2, and His-57.CD2 sees its ASA augment by 20%. These results would, therefore, suggest that His-57 constitutes the most likely candidate as an electron donor so as to rationalize our IMAC results (see also Figure 3).

Active-Site-Specific Chemical Modification of His-57. To directly assess His-57 participation in IMAC, we decided to call on using the unique specificity of covalent inhibitors of CHA, the rationale behind this being that chemical modification of His-57 with TPCK (Schoellman & Shaw, 1963) or MNBS (Nakagawa & Bender, 1970) should abolish CHA binding to IDA−Cu(II). Following reaction with either TPCK or MNBS, over 95% of the enzymatic activity is lost, consistent with an effective chemical modification of active site His-57. Unexpectedly, however, both modified enzymes are found to behave similarly to native CHA in IMAC−IDA−Cu(II) (data not shown). Therefore, this finding casts doubts on the participation of His-57 in the IMA recognition event and, taken together with the ASA calculations, further suggests the occurrence of an alternative recognition mechanism that may not involve histidines.

Novarose−IDA−Cu(II) Binding Studies and pH Titration. To gather a better understanding of α-chymotrypsin interactions with IDA−Cu(II), we analyzed both its binding affinity and pH dependence. Nonchromatographic equilibrium binding experiments were hence performed as described by Hutchens (Hutchens & Yip, 1990), under the conditions used in the present study for the chromatographic separation of chymotrypsin subspecies. Binding data analysis according to Scatchard (1949) is consistent with the existence of a single class of binding site with $K_d = 37$ μM (Figure 2). A similar value ($K_d = 81$ μM) had already been obtained by Hutchens and Yip using Chelating Sepharose Fast Flow−IDA−Cu(II) with a sodium phosphate buffer at pH 7 (Hutchens & Yip, 1990).

pH titration of α-chymotrypsin binding to Novarose−IDA−Cu(II) was done by isocratic elution at various pH values as previously described (Sulkowski, 1987). An abrupt transition in protein retention is observed as the pH is increased from 6.0 to 6.25 and even more so in going from pH 6.25 to pH 6.5. This behavior is consistent with the titration of a protein site with a pK_a near 6.5 (Figure 2B; the α/γ-chymotrypsin peak is indicated by an arrow). This pK_a value for a solvent-exposed chemical group agrees best with that of a histidine side chain. Given that the participation of His-57 has already been excluded, the data would therefore now suggest that, despite its low static accessibility, His-40 is the residue implicated, all the more so since a measurable contribution from residues other than histidine is rather unlikely. This is based on the fact that at the pH (7.5) used in our experiment, the participation of terminal amino groups remains minor in proteins (Andersson & Sulkowski, 1992; Johnson et al., 1996) and probably further reduced here because of the potential competition with the amino group present in the buffer (Tris-HCl; pK_a = 8.06 at 25 °C; Perrin & Dempsey, 1987) used during chromatography. Moreover, negatively charged carboxylate groups of aspartates and glutamates cannot be considered as potential ligands to IDA−Cu(II) near neutral pH due to repulsion effects with the overall negatively charged copper−chelate matrix (Sulkowski, 1987; Vijayalakshmi, 1989; Mrabet, 1992).

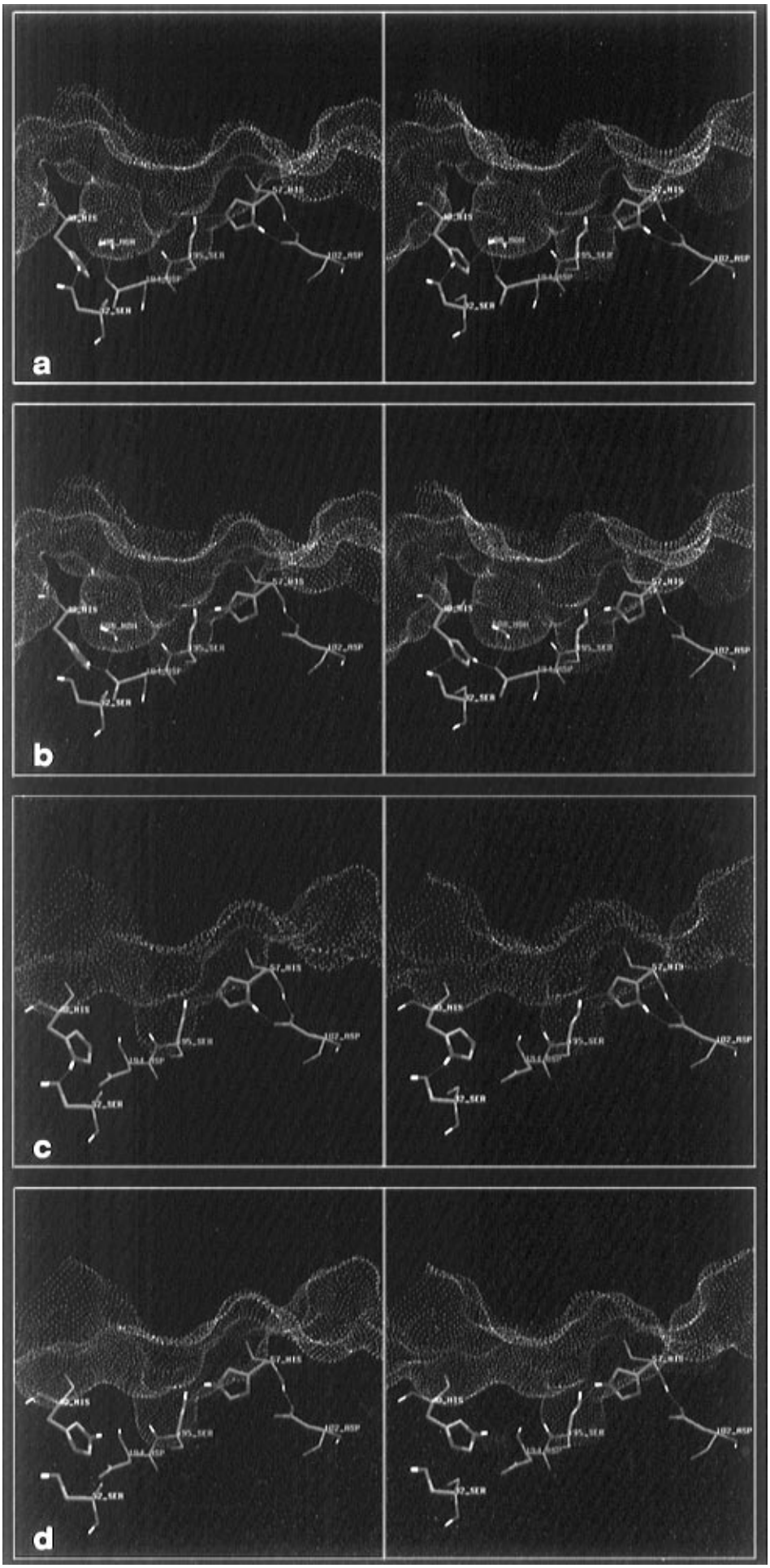
a
b
c
d

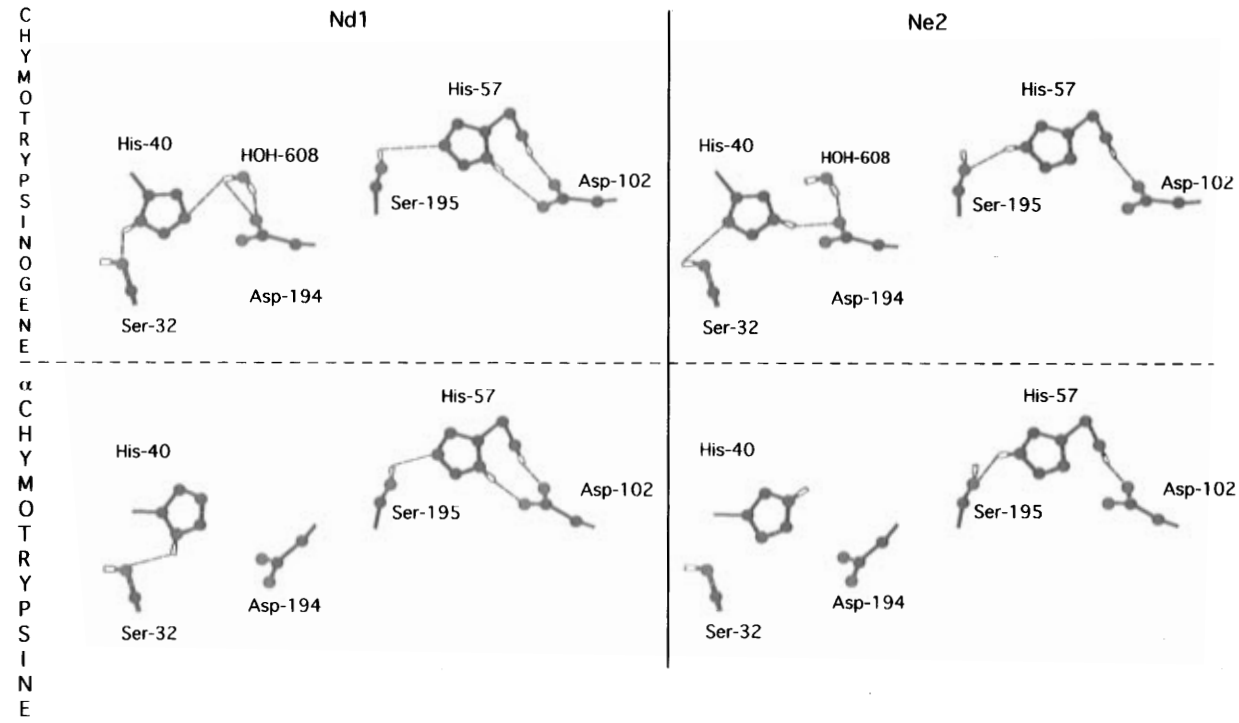

FIGURE 3: Hydrogen-bonding interactions and accessible surface areas of His-40 and His-57 in bovine chymotrypsinogen and α-chymotrypsin. Panel A (left page): Stereoviews of the hydrogen bonds in chymotrypsinogen involving both His-40 and His-57 in either the ND1-protonated form (a) or the NE2-protonated form (b) and in α-chymotrypsin involving both His-40 and His-57 in either the ND1-protonated form (c) or the NE2-protonated form (d). The structures are taken from monomers A in the Brookhaven PDB (Bernstein et al., 1977), entries 2CGA (bovine pancreatic chymotrypsinogen; Wang et al., 1985) and 5CHA (bovine α-chymotrypsin; Blevins & Tulinsky, 1985), after steepest descent energy minimization (Levitt & Lifson, 1969) to optimize geometry. For the sake of clarity, a 15 Å thick (for 2CGA) or a 20 Å thick (for 5CHA) slice of the corresponding protein is shown with only the residues of interest, and water 608 of 2CGA where applicable, while nonpolar hydrogen atoms have been omitted; side chains and water 608 are in heavy bold; main-chain atoms are shown in light bold. Carbon atoms are shown in green, nitrogens in blue, oxygens in red, and polar hydrogens in white. The red dashed lines represent the hydrogen bonds made by His-40 and His-57. All-hydrogen atom molecules were constructed using the BRUGEL molecular modeling package (Delhaise et al., 1984; UsrConsult, Louvain-la-Neuve, Belgium). The Connolly (1983) dot surface represents the protein (heteroatoms, hence water 608, have been excluded from the surface computation) surface accessible to the spherical probe with a 1.93 Å radius (Mrabet, 1992); the accessible surface specifically contributed by the atoms of His-40 and His-57 is decorated in red. Note that the protein core lies below the Connolly surface, while the solvent region is above it. All figures were generated in the relaxed mode with BRUGEL (Delhaise et al., 1984; UsrConsult, Louvain-la-Neuve, Belgium). Panel B (above): Schematic representation of the hydrogen bonds in chymotrypsinogen involving both His-40 and His-57 in either the ND1-protonated form (a) or the NE2-protonated form (b) and in α-chymotrypsin involving both His-40 and His-57 in either the ND1-protonated form (c) or the NE2-protonated form (d).

Side-Chain Flexibility in Chymotrypsinogen and α-Chymotrypsin: B Factors and Hydrogen Bonding. In an attempt to resolve the apparent contradiction of the data from chemical modification and binding studies with the static ASA calculations, the isotropic temperature factors, B —available only for the chymotrypsinogen A structure (2CGA) (Wang et al., 1985), were examined. These indicate that the flexibility of the imidazole group of His-40 is significantly higher [$B = 33.3 \pm 4.26$ Å^2/atom; mean per monomer in the "two-monomers-per-unit-cell" crystal structure ± 1 SD] than that of His-57 [$B = 11.5 \pm 2.4$ Å^2/atom]. If an increase in side-chain flexibility is to correlate with its ability to "snatch" the IDA−Cu(II) ligand, then one may expect that the distinction between His-40 and His-57 would become even more remarkable in CHA, since the mature enzyme displays a higher affinity to the metal−chelate complex. In the absence of published B factors for the CHA structure, we relied on comparing the hydrogen-bonding characteristics of CGA and CHA.

At neutral pH, the imidazole side chain of histidine can exist in two tautomeric forms, the ND1-protonated form or the NE2-protonated form (Reynolds et al., 1973). Histidine hydrogen bonding in either configuration was analyzed for both monomers present in the crystal unit in both CGA and CHA. Table 2 shows that regardless of the chosen tautomer, zymogen activation is accompanied by a loss of hydrogen bonds (H-bonds) for His-40 but not for His-57. As an example, in the "dimeric" crystal structure of CGA, ND1-protonated His-40 makes a total of four H-bonds, one to Ser-32.OG and a water-mediated H-bond to Asp-194.OD1 in both monomers A and B (Figure 3a, panel A). Upon zymogen maturation, the latter interaction which involves the His-40.NE2 unprotonated nitrogen atom is lost, hence making this atom free to engage in other interactions (Figure 3c, panel A). With NE2 protonation His-40 makes a H-bond to Asp-194.OD1 in both monomers of CGA (Figure 3b, panel A). This H-bond is lost in CHA (Figure 3d, panel A) and replaced by an uncharged H-bond to main-chain Gly-193.O in monomer A only (not shown). Since chymotrypsins are known to exist as monomers in solutions of high ionic strength above pH 5 (Wilcox, 1970); (these premises are all satisfied by our experimental conditions), these data indicate that on a monomer basis the latter interaction occurs only 50% of the time. In contrast, not only is the hydrogen bonding of His-57 maintained during the activation process but, further, new H-bonds are now established between His-57.HE2 and Ser-195.OG in monomer B with the NE2-protonated His-57 form or, for the ND1-protonated tautomer,

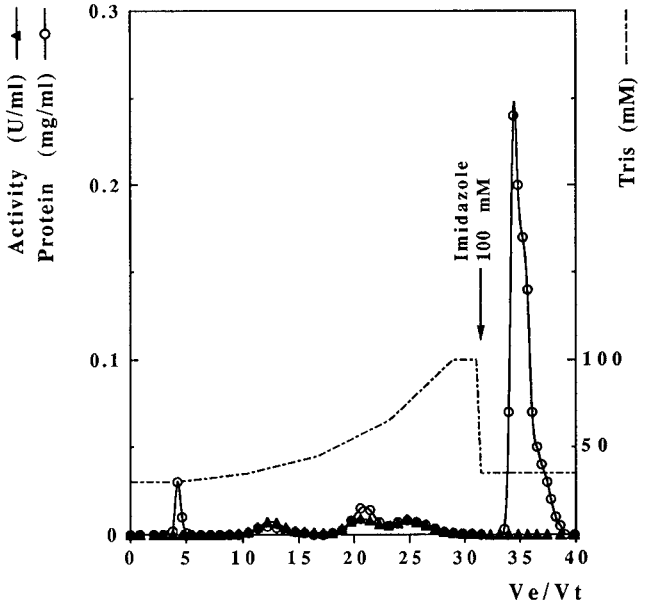

FIGURE 4: IMAC on Novarose−IDA−Cu(II) of DFP- and PMSF-modified chymotrypsins. Active site Ser-195 was affinity labeled with PMSF as described previously (Farhney & Gold, 1963). Excess reagent was removed by desalting prior to IMAC. In each case, inhibition reached at least 95% completion and was maintained even after the chromatographic run. DFP-treated α-chymotrypsin (C1012, lot 54F8145) was purchased directly from Sigma Chemical Co. (St. Louis, MO). Following chemical modification with either DFP or PMSF, the resulting proteins display a markedly increased retention onto Novarose−IDA−Cu(II) since elution requires 100 mM imidazole. In contrast, chymotrypsins affinity labeled at His-57 with TPCK or MNBS show retention profiles indistinguishable from that of untreated chymotrypsin.

also in monomer B, between His-57.NE2 and Ser-195.HG and between His-57.HD1 and Asp-102.OD2. These data, schematized in Figure 3, panel B, thus suggest that because of opposite changes in hydrogen bonding, the flexibility difference between His-40 and His-57 is even more pronounced as a result of zymogen maturation to α-chymotrypsin. The data in Table 2 further suggest that the change in the hydrogen-bonding status should even be amplified, would either histidine exist in the charged, double protonated form.

Specific Chemical Modification of Active Site Ser-195. If H-bonds are indeed "burying" the otherwise surface-accessible His-57, then disrupting the hydrogen-bonding network that implicates His-57 should reverse this situation. Using ^{15}N NMR, Bachovchin demonstrated earlier that treatment with the active site serine-specific reagents, PMSF or DFP, of a closely related serine protease, the α-lytic protease, results in breaking the catalytic triad His−Ser H-bond (Bachovchin, 1986). Sulkowski (1987) also observed that Ser-195 chemical modification with DFP enhanced chymotrypsin retention on chelating Sepharose−IDA−Cu(II). Similarly, we observe that specific chemical modification of catalytic Ser-195 in α-chymotrypsin with either PMSF or DFP produces a significantly large increase in IMAC−IDA−Cu(II) retention of the enzyme, since the desorption of the modified protein can only be achieved at high imidazole concentration (100 mM; Figure 4). Consistent with a hydrogen bond breaking mechanism within the active site, this finding is a strong suggestion for the additional participation of the newly freed His-57 in the IDA−Cu(II) adsorption event.

Taking all the data together, we therefore propose the following: (i) Even though His-57 displays a higher *static* accessibility than His-40 in the protein crystal structures, its being engaged in multiple hydrogen bonds with its neighbors of the catalytic triad prohibits its interaction with IDA−Cu-(II). In support of this hypothesis, we expectedly observe that disruption of the His-57/Ser-195 hydrogen bond by site-specific chemical modification of the catalytic serine brings about an increased affinity to IDA-Cu(II). (ii) Despite its low *static* accessibility, the His-40 side chain is flexible enough to become more accessible on the protein surface as a direct consequence of H-bond loss upon zymogen maturation and, hence, able to establish a coordination bond to IDA−Cu(II). It is clearly significant that the occurrence of such a protein dynamics event cannot be predicted on the basis of structural analysis of the X-ray crystallographic models alone. (iii) Finally, in line with our working hypothesis, it must be stressed that progressive loss of H-bonds involving His-40 is expected to occur with a concomitant decrease of the pK_a of the residue side chain; this, in turn, would provide a plausible molecular mechanism to account for the modification of the electron-donating strength displayed by chymotrypsin subspecies as maturation proceeds, as it is indeed illustrated by the correlated increase in affinity toward IDA−Cu(II). In further support of our contention, it is worthwhile mentioning that a decrease in His-40 pK_a from 8 in CGA (Cruickshank & Kaplan, 1975) to 6.8−7.2 in CHA (Cruickshank & Kaplan, 1975; Markley & Ibanez, 1978) has indeed been reported previously.

CONCLUSIONS

In the present study, an interactive combination of IMAC, conventional protein biochemistry techniques, and molecular modeling is shown to provide novel insights into the structural and physicochemical basis for molecular recognition. Histidine residues are described as exquisite reporter groups of minute protein conformational changes which are not evident from simple examination of a static three-dimensional protein model as derived from X-ray crystallography analysis. Moreover, the computation of static accessibility alone may not suffice to unequivocally identify protein sites for ligand recognition. In this regard, the H-bonding status is likely to play a prominent role on at least three levels. First, H-bonds will undoubtedly reduce the accessible surface area of the atoms involved; this aspect will obviously be overlooked whenever accessibility studies are performed on protein models without explicit hydrogen atoms by using "isotropic" united atom radii as it is the "rule" now. Second, H-bond interactions will curtail the electron-donating properties of the nitrogen atom and therefore make it a poor metal ligand. Third, if residue flexibility is also required in order for the protein to interact with a ligand, then the interference brought about by H-bond stabilization of the concerned residue becomes evident.

We must stress that, in the present study, although we have been able to provide several strong and correlated arguments to suggest the implication of α-chymotrypsin His-40 in IDA−Cu(II) recognition and binding, it remains to be directly demonstrated. The absence of a specific chemical modification reaction of His-40 that also yields a stable product under our experimental conditions has precluded the direct control of its participation [see Melchior and Fahrney (1970)]. To settle this issue would require assessing the role of His-40 by means of genetic engineering techniques. Nevertheless,

as discussed above, it remains that the involvement of residues other than histidine appears not plausible under our experimental conditions, and this assertion is in agreement with a large body of evidence available on the interaction of proteins with metal chelates near neutral pH (Sulkowski, 1985, 1987, 1989; Arnold, 1991; Mrabet, 1992; Johnson et al., 1996).

Nonetheless, the most significant outcome of our study remains the demonstration that the active site His-57 in bovine chymotrypsin, although well exposed on the protein surface, is unable to engage in coordination−bond formation to immobilized IDA−Cu(II). This apparent conflict with the current principles used to rationalize molecular interactions in IMAC could, however, be reconciled by showing that His-57 is engaged in a strong and stable hydrogen-bonding network in unliganded chymotrypsin, even under our experimental conditions of high ionic strength (1.0 M NaCl). The strength of such hydrogen-bonding interactions should further be high enough to provide for the absence of an effective competitive effect by IDA−Cu(II), even under the high metal−chelate density conditions of our experimental setting.

Our study hence further opens a wider perspective on the analysis of the histidine microenvironment in enzyme active sites where this residue is ubiquitous. This is especially true for the serine protease family where histidine engagement in hydrogen bonding has so far remained a matter of debate (Jordan & Polgar, 1981; Bachovchin, 1985, 1986; Smith et al., 1989; Bartunik et al., 1989; Derewenda et al., 1994; Frey et al., 1994; Tobin et al., 1995) which is ultimately likely to have profound implications on our understanding of mechanistic aspects of catalysis.

ACKNOWLEDGMENT

We thank Dr. E. Sulkowski for his sustained interest and stimulating discussions and Dr. G. Lindgren, Inovata AB, Sollentuna, Sweden, for the gracious gift of the Novarose Act^{High}-100/40. The computer equipment and software used for molecular modeling in this study was made available by the Service Commun de Biophysicochimie des Interactions Moléculaires, Faculté des Sciences, Université Henri Poincaré−Nancy I, Vandœuvre-lès-Nancy, France.

REFERENCES

Alard, P. (1991) Ph.D. Dissertation, Université Libre de Bruxelles, Brussels, Belgium.
Alard, P., & Wodak, S. J. (1991) *J. Comput. Chem. 12*, 918−922.
Andersson, L., & Sulkowski, E. (1992) *J. Chromatogr. 604*, 13−17.
Arnold, F. (1991) *BioTechnology 9*, 151−156.
Bachovchin, W. W. (1985) *Proc. Natl. Acad. Sci. U.S.A. 82*, 7948−7951.
Bachovchin, W. W. (1986) *Biochemistry 25*, 7751−7759.
Bartunik, H. D., Summers, L. J., & Bartsch, H. H. (1989) *J. Mol. Biol. 210*, 813−828.
Bernstein, F. C., Koetzle, T. F., Williams, G. J. B., Meyer, E. F., Jr., Brice, M. D., Rodgers, J. R., Kennard, O., Shimanouchi, T., & Tasumi, M. (1977) *J. Mol. Biol. 112*, 535−542.
Blevins, R. A., & Tulinsky, A. (1985) *J. Biol. Chem. 260*, 4264−4275.
Botros, H. G., & Vijayalaksmi, M. (1989) *J. Chromatogr. 495*, 113−122.
Bradford, M. M. (1976) *Anal. Biochem. 72*, 248−254.
Brooks, A., Bruccoleri, R. E., Olafson, B. D., States, D. J., Swaminathan, S., & Karplus, M. (1983) *J. Comput. Chem. 4*, 187−217.
Connolly, M. L. (1983) *Science 221*, 709−713.
Corradini, D., El Rassi, Z., Horvath, C., Guerra, G., & Horne, W. (1988) *J. Chromatogr. 458*, 1−11.
Cruickshank, W. H., & Kaplan, H. (1975) *Biochem. J. 147*, 411−416.
Delhaise, P., Bardiaux, M., & Wodak, S. J. (1984) *J. Mol. Graphics 2*, 103−106.
Derewenda, Z. S., Derewenda, U., & Kobos, P. M. J. (1994) *J. Mol. Biol. 241*, 83−93.
Dixon, M. M., & Matthews, B. W. (1989) *Biochemistry 28*, 7033−7038.
Dreyer, W. J., & Neurath, H. (1955) *J. Biol. Chem. 217*, 527−534.
Fahrney, D. E., & Gold, A. M. (1963) *J. Am. Chem. Soc. 85*, 997−1000.
Fazakerley, S., & Best, D. R. (1965) *Anal. Biochem. 12*, 290−295.
Frey, P. A., Whitt, S. A., & Tobin, J. B. (1994) *Science 264*, 1927−1930.
Harel, M., Su, C. T., Frolow, F., Silman, S., & Sussman, J. L. (1991) *Biochemistry 30*, 5217−5225.
Hemdan, E. S., Zhao, Y. J., Sulkowski, E., & Porath, J. (1989) *Proc. Natl. Acad. Sci. U.S.A. 86*, 1811−1815.
Hubert, P., & Porath, J. (1981) *J. Chromatogr. 206*, 164−168.
Hummel, B. C. W. (1959) *Can. J. Biochem. Physiol. 37*, 1393−1399.
Hutchens, T. W., & Yip, T. T. (1990) *Anal. Biochem. 191*, 160−168.
Johnson, R. D., Todd, R. J., & Arnold, F. H. (1996) *J. Chromatogr. 725*, 225−235.
Lee, B., & Richards, F. M. (1971) *J. Mol. Biol. 55*, 379−400.
Levitt, M., & Lifson, S. (1969) *J. Mol. Biol. 46*, 269−279.
Liu, Y., & Yu, S. (1990) *J. Chromatogr. 515*, 169−173.
Markley, J. L., & Ibanez, I. B. (1978) *Biochemistry 17*, 4627−4639.
McDonald, I. K., & Thornton, J. M. (1994) *Protein Eng. 8*, 217−224.
Melchior, W. B., & Fahrney, D. (1970) *Biochemistry 9*, 251−258.
Mrabet, N. T. (1992) *Biochemistry 31*, 2690−2702.
Nakagawa, Y., & Bender, M. L. (1970) *Biochemistry 9*, 259−264.
Nakagawa, Y., Yip, T.-T., Belew, M., & Porath, J. (1988) *Anal. Biochem. 168*, 75−81.
Perrin, D. D., & Dempsey, B. (1987) in *Buffers for pH and Metal Ion Control*, p 57, Chapman & Hall Ltd., London.
Porath, J., Carlsson, J., Olsson, I., & Belfrage, G. (1975) *Nature 258*, 598−599.
Reynolds, W. F., Peat, I. R., Freedman, M. H., & Lyerla, J. R., Jr. (1973) *J. Am. Chem. Soc. 95*, 328−331.
Rovery, M., Poilroux, M., Curnier, A., & Desnuelle, P. (1955) *Biochim. Biophys. Acta 17*, 565−572.
Scatchard, G. (1949) *Ann. N.Y. Acad. Sci. 51*, 660−672.
Schoellmann, G., & Shaw, E. (1963) *Biochemistry 2*, 252−255.
Schwert, G. W., & Takenaka, Y. (1955) *Biochim. Biophys. Acta 6*, 570−578.
Smith, S. O., Farr-Jones, S., Griffin, R. G., & Bachovchin W. W. (1989) *Science 244*, 961−964.
Sulkowski, E. (1985) *Trends Biotechnol. 3*, 1−7.
Sulkowski, E. (1987) in *Protein Purification: Micro to Macro* (Burgess, R. R., Ed.) pp 149−162, Alan R. Liss Inc., New York, NY.
Sulkowski, E. (1989) *BioEssays 10*, 170−175.
Tobin, J. B., Whitt, S. A., Cassidy, C. S., & Frey, P. A. (1995) *Biochemistry 34*, 6919−6924.
Vijayalakshmi, M. A. (1989) *Trends Biotechnol. 7*, 71−76.
Wang, D., Bode, W., & Huber, R. (1985) *J. Mol. Biol. 185*, 595−624.
Wilcox, P. E. (1970) *Methods Enzymol. 19*, 64−108.
Wodak, S. J., van Belle, D., & Prevost, M. (1995) in *Computer Modelling in Molecular Biology* (Goodfellow, J. M., Ed.) pp 61−102, VCH, Weinheim, Germany.
Zhao, Y. J., Sulkowski, E., & Porath, J. (1991) *Eur. J. Biochem. 202*, 1115−1119.

BI9618070